Tailored mixing inside a translating droplet

R. Chabreyrie[1], D. Vainchtein[2,3], C. Chandre[4], P. Singh[5], N. Aubry[1]
[1] *Mechanical Engineering Department, Carnegie Mellon University, PA 15213, USA*
[2] *School of Physics, Georgia Institute of Technology, GA 30332, USA*
[3] *Space Research Institute, Moscow, GSP-7, 117997, Russia*
[4] *Centre de Physique Théorique, Luminy-case 907, F-13288 Marseille cedex 09, France*
[5] *Mechanical Engineering Department, New Jersey Institute of Technology, Newark, NJ 07102, USA*
(Dated: October 25, 2007)

Tailored mixing inside individual droplets could be useful to ensure that reactions within microscopic discrete fluid volumes, which are used as microreactors in "digital microfluidic" applications, take place in a controlled fashion. In this letter we consider a translating spherical liquid drop to which we impose a time periodic rigid-body rotation. Such a rotation not only induces mixing via chaotic advection, which operates through the stretching and folding of material lines, but also offers the possibility of tuning the mixing by controlling the location and size of the mixing region. In particular, complete mixing can be induced. Tuned mixing is obtained by judiciously adjusting the amplitude and frequency of the rotation, which are determined by using a resonance condition and following the evolution of adiabatic invariants.

PACS numbers: 47.51.+a, 47.61.Ne, 47.52.+j

Droplets have been proposed as an alternative to standard fluid-stream microfluidics for lab-on-a-chip applications. This microfluidics approach, also referred to as "digital" because it uses "discrete" fluid volumes (droplets) rather than continuous streams, holds great promise due to the possibility of using single droplets as microreactors [1]. Efficient mixing, however, is needed for reactions to occur, but remains difficult to achieve because the Reynolds number is usually very small and the flow laminar. This issue has recently attracted much attention in the literature. For flows in microchannels, while many strategies consist in altering the channel geometry, the use of external forcing alone has also proved to be efficient (see, e.g., [2–6]). For droplet-based microfluidics, the forcing is the preferred strategy as the deformation of the droplet is difficult to control. In almost all cases, the enhancement of mixing in miniature geometries is based on the principle of chaotic advection, the stirring phenomenon that stretches and folds fluid elements in order to significantly increase the interfacial area between the two fluids to be mixed.

Chaotic advection inside a liquid drop suspended in a low Reynolds number flow and subjected to a forcing has been studied extensively [7–11]. In this letter, we focus on unsteady – yet periodic – forcing. From a dynamical systems viewpoint, the introduction of a time-dependent perturbation or forcing breaks the invariants (related to the symmetries of the unperturbed system), thus introducing resonances between the natural frequencies of the unperturbed problem and the frequency(-ies) of the forcing [12]. Although such resonances create chaotic regions where mixing occurs, in general, chaotic and regular regions co-exist.

In many situations where it is indeed possible to create chaos, controlling the mixing region(s) remains a challenge. Such a control, however, should be possible since a chaotic system is sensitive to changes in parameter values (as it is to changes in initial conditions). These changes generically modify the resonances so that the location of the chaotic regions may vary, while also affecting the size of the chaotic regions.

Our general approach to this issue is to consider a bounded three-dimensional (3D) flow, which is the superposition of an integrable flow $\mathbf{v}_0$ with at least one invariant (associated with the particular symmetries of the considered flow geometry) and a small time-dependent perturbation $\varepsilon\mathbf{v}_1(\mathbf{x},t)$, $0 \leq \varepsilon \ll 1$. If $\mathbf{v}_0$ has only one invariant, the phase space contains two-dimensional tori whose nonlinear stability with respect to perturbations is ensured by the KAM theorem. In this case, the perturbed flow, $\dot{\mathbf{x}} = \mathbf{v}_0(\mathbf{x}) + \varepsilon\mathbf{v}_1(\mathbf{x},t)$, has poor mixing properties if the amplitude of the perturbation ε is small, since two-dimensional tori act as barriers to chaotic diffusion (see, e.g., [13]). If, on the other hand, $\mathbf{v}_0$ has two invariants, trajectories of this integrable flow are all periodic. Most of these periodic orbits are expected to be broken by a generic perturbation $\mathbf{v}_1$ with an arbitrarily small amplitude ε. Efficient mixing properties might then be obtained with such perturbed flows. In this work, we consider an axisymmetric integrable flow possessing two invariants, thus possibly offering efficient mixing properties after being perturbed.

While many previous works [7, 8, 14, 15] have shown the existence of chaotic behavior in 3D bounded steady flows, we turn our attention to 3D unsteady flows; the added unsteadiness considered here targets the control of the chaotic behavior through resonance phenomena [16].

Specifically, we consider a spherical liquid drop immersed in an incompressible Newtonian flow in the case where the linear external field is characterized by translational velocity and vorticity vectors, similarly to [8]. As in the latter reference, we assume that the local Reynolds

number is much smaller than one and that the interfacial tension is sufficiently large for the drop to remain spherical. The internal velocity field is obtained by solving the Stokes flow problem for both the internal and external flows satisfying the continuity of velocity and tangential stress conditions across the drop surface. In addition, we introduce unsteadiness in the problem by making the vorticity time dependent. In a Cartesian coordinate system translating with the center-of-mass velocity of the drop, and with the z axis aligned with the direction of the translation, the fluid particle paths are given by the solution of the non-autonomous dynamical system:

$$\begin{aligned} u = \dot{x} &= zx - a(t)\omega_z y, \\ v = \dot{y} &= zy + a(t)\left(\omega_z x - \omega_x z\right), \\ w = \dot{z} &= (1 - 2x^2 - 2y^2 - z^2) + a(t)\omega_x y, \end{aligned} \tag{1}$$

where all lengths and velocities have been non-dimensionalized by the drop radius and the magnitude of the translational velocity. Here, the vorticity is defined by $\boldsymbol{\omega}(\omega_x, \omega_y, \omega_z) = (1/\sqrt{2}, 0, 1/\sqrt{2})$, the unitary vector corresponding to the axis of rotation, and $a(t) = \varepsilon/2\,(1 + \cos\omega t)$, characterized by the frequency ω and the amplitude ε. In this letter, we consider only small amplitudes, i.e. for $0 \leq \varepsilon \ll 1$. Note that the former equations are identical to those in [8] where the constant vorticity vector has been replaced by $a(t)\boldsymbol{\omega}$. This can be done by either assuming unsteady vorticity in the external flow field, or by applying a time dependent body force. In practice, this could be realized, e.g., by creating a time dependent swirl motion in the external flow or by applying an electric field that exerts a torque on the drop [17]. The resulting flow is the superposition of a Hill's vortex and an unsteady rigid body rotation, and the surface of the drop, $r^2 = x^2 + y^2 + z^2 = 1$, is invariant under the flow (1).

We now discuss some features of the unperturbed axisymmetric (and thus two-dimensional (2D)) flow ($\varepsilon = 0$). The flow possesses two independent integrals of motion, e.g., the streamfunction ψ and the azimuthal angle ϕ such that

$$\psi = 1/2\rho^2\left(1 - r^2\right), \quad \phi \arctan y/x, \tag{2}$$

where $\rho^2 = x^2 + y^2$ and $\psi \in [0, 1/8]$. The streamlines of the unperturbed system are lines of constant ψ and ϕ, denoted by $\Gamma_{\psi,\phi}$, and defined as $(1-2\rho^2)^2 + (2\rho z)^2 = 1 - 8\psi$ (see Fig. 1). Almost all streamlines are closed curves surrounding a circle of degenerate elliptic fixed points ($\rho = 1/\sqrt{2}, z = 0$). In addition, there are two hyperbolic fixed points located at the poles of the sphere which are connected by heteroclinic orbits. The frequency of the motion on $\Gamma_{\psi,\phi}$ is given by

$$\frac{2\pi}{\Omega(\psi)} = \int_{-\pi/2}^{\pi/2} \frac{\sqrt{2}\,\mathrm{d}\alpha}{\sqrt{1 + \gamma(\psi)\sin\alpha}} = \frac{2\sqrt{2}}{\sqrt{1+\gamma}} K\left(\sqrt{\frac{2\gamma}{1+\gamma}}\right), \tag{3}$$

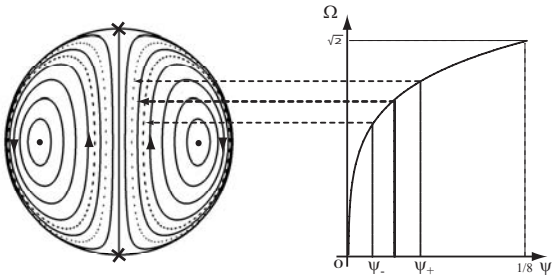

FIG. 1: (a) Flow inside the droplet without rotation. (b) Frequency $\Omega(\psi)$ of Hill's spherical vortex as given by Eq. (3).

where $\gamma(\psi) = \sqrt{1 - 8\psi}$ and K is the complete elliptic function of the first kind. The frequency Ω is bounded by two limits, $\Omega(0) = 0$ and $\Omega(1/8) = \sqrt{2}$ (see Fig. 1).

On every streamline $\Gamma_{\psi,\phi}$, we introduce a uniform phase $\chi \mod(2\pi)$ such that $\chi = 0$ on the $x - y$ plane (with $\rho \leq 1/\sqrt{2}$) and $\dot{\chi} = \Omega(\psi)$. The unperturbed system, which can be rewritten in terms of (ψ, ϕ, χ) as

$$\dot{\psi} = 0, \quad \dot{\phi} = 0, \quad \dot{\chi} = \Omega(\psi),$$

belongs to the class of action-action-angle flows.

In the perturbed case $0 < \varepsilon \ll 1$, the time evolution of the two invariants of the unperturbed system is given by

$$\begin{aligned} \dot{\psi} &= -2a(t)w_x\psi\sin\phi G(\psi,\chi), \\ \dot{\phi} &= a(t)w_z - a(t)w_x\cos\phi G(\psi,\chi), \end{aligned} \tag{4}$$

where $G(\psi, \chi) = z/\rho$ is 2π periodic in χ and has zero average in χ. The time evolution equation for χ is

$$\dot{\chi} = \Omega(\psi) + a(t)H(\psi, \phi, \chi), \tag{5}$$

where H is 2π periodic in χ. The dynamics possesses two distinct time scales, a fast one (which changes on a time scale of order one) which is associated with χ, and a slow one (which changes on a time scale of order $1/\varepsilon$) associated with ψ and ϕ.

If Ω and ω are incommensurate, then the averaging over Ω and over ω can be performed independently. In this case, the time-periodic terms in Eq. (4) average out, and the *averaged system* reduces to

$$\dot{\psi} = 0, \quad \dot{\phi} = -\varepsilon/2.$$

Thus in the averaged system, the value of ψ is conserved as it was in the unperturbed system; in other words, ψ is an invariant of the averaged system. Each trajectory of the averaged system evolves on two-dimensional nested tori $\mathcal{T}_\psi$. In the perturbed system, ψ is an adiabatic invariant and the motion follows adiabatically the tori $\mathcal{T}_\psi$.

We now turn to the generation of a 3D chaotic mixing region inside the drop, for which we seek to control both the location and the size. The strategy used for this

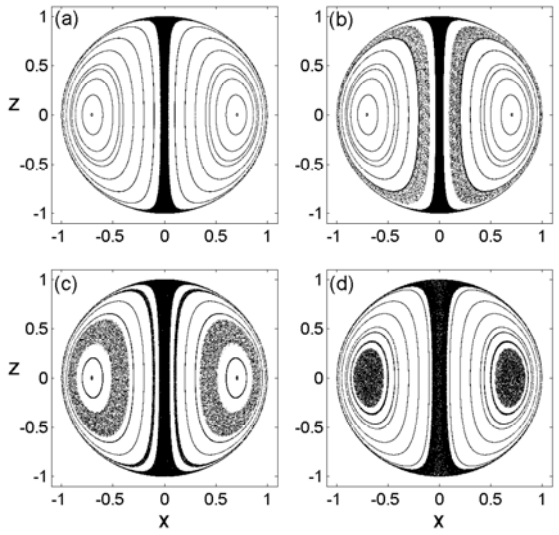

FIG. 2: Liouvillian sections for the amplitude $\varepsilon = 0.03$ and the frequencies (a) $\omega = 0.55$, (b) $\omega = 0.93$, (c) $\omega = 1.28$, (d) $\omega = 1.41$. The dash line inside the CMR is the torus $\mathcal{T}^{(1)}$.

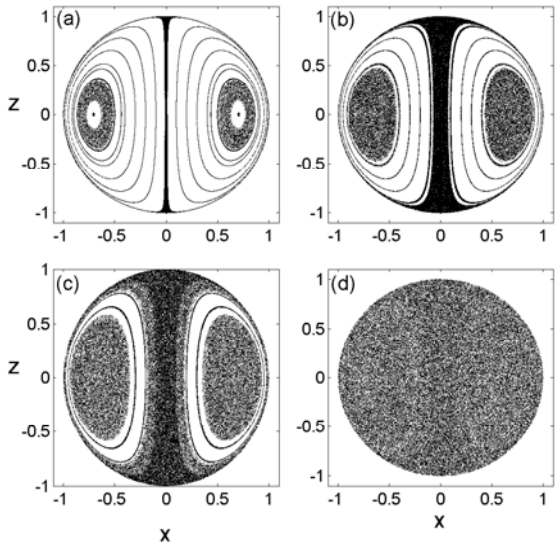

FIG. 3: Liouvillian sections for the frequency $\omega = 1.376$ and the amplitudes (a) $\varepsilon = 0.01$, (b) $\varepsilon = 0.05$, (c) $\varepsilon = 0.10$, (d) $\varepsilon = 0.20$.

purpose is to bring a chosen family of unperturbed tori $\mathcal{T}_\psi$ into resonance with the perturbation $a(t)$ by adjusting the frequency ω to satisfy the resonance condition

$$n\Omega(\psi) - \omega = 0, \tag{6}$$

for some $n \in \mathbb{N}$ (see Fig. 1). For any fixed ω we denote by $\left\{\mathcal{T}^{(n)}(\omega) \;|n \in \mathbb{N}\right\}$ the set of resonant tori $\mathcal{T}_\psi$ satisfying (6). Hereafter, we denote by CMR the chaotic mixing region generated around $\mathcal{T}^{(1)}(\omega)$.

Figures 2 and 3 present characteristic views of the perturbed system in the form of *Liouvillian sections*, which consist of 2D projections of time-periodic 3D flows by a combination of a stroboscopic map and a Poincaré section (in our case, the $y = 0$ plane). Figure 2 shows that time periodic perturbations $a(t)$ create a 3D CMR around each $\mathcal{T}^{(1)}(\omega)$ and its location is controlled by varying ω according to Eq. (6). In what follows, we analyze the location and the size of the CMR as a function of ω and ε.

For small values of ω, all the resonances are located near the pole-to-pole heteroclinic connections (at $\psi = 0$, near the z axis and near the boundaries of the drop, see Fig. 2a). As ω is increased, the CMR penetrates deeper into the drop (Fig. 2b). In the interval $0 < \omega < \sqrt{2}$, the CMR is the largest chaotic region (compared to chaotic regions corresponding to higher order resonances), with all the other chaotic regions localized close to the z axis and near the drop boundaries (around the heteroclinic orbits); this is due to the shape of $\Omega(\psi)$. As ω is increased further, the CMR moves toward the location of the elliptic fixed points of the unperturbed system, following very accurately the location of the resonant torus $\mathcal{T}^{(1)}(\omega)$ (Fig. 2c). As the value of ω approaches $\sqrt{2}$, the CMR shrinks to the circle of elliptic fixed points (Fig. 5).

Whereas the frequency ω of the rigid body rotation is mostly responsible for the location of the CMR, it is its amplitude ε which mostly determines its size. Figure 3 shows that the size of the chaotic mixing regions created by the $n = 1$ resonance and by higher order resonances (mostly the $n = 2$ resonance) increases as the amplitude of the perturbation increases. Around $\varepsilon \approx 0.20$, the chaotic regions around the heteroclinic orbits and the CMR join together to cover the entire drop volume (complete mixing). In the averaged system, recall that the

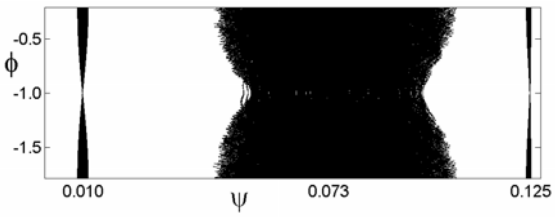

FIG. 4: Projection of three characteristic trajectories on the slow phase plane, for three initial conditions for which $\phi_0 = 0.000$ and ψ takes the values: $\psi_0 = 0.010;\ 0.073;\ 0.125$.

adiabatic invariant ψ is constant. In the non-averaged system, however, along a given trajectory starting at $\psi = \psi_0$ it varies between $\psi^-(\psi_0;\omega,\varepsilon)$ and $\psi^+(\psi_0;\omega,\varepsilon)$. The width $\Delta\psi = \psi^+(\psi_0;\omega,\varepsilon) - \psi^-(\psi_0;\omega,\varepsilon)$ is small away from the resonance, and increases significantly closer to the resonance. The projection of three characteristic trajectories onto the (ψ,ϕ)-plane (called the *slow plane* in the theory of dynamical systems) is presented in Fig. 4. The narrow black regions on the right and on the left are off-resonance trajectories, that stay quite close to the

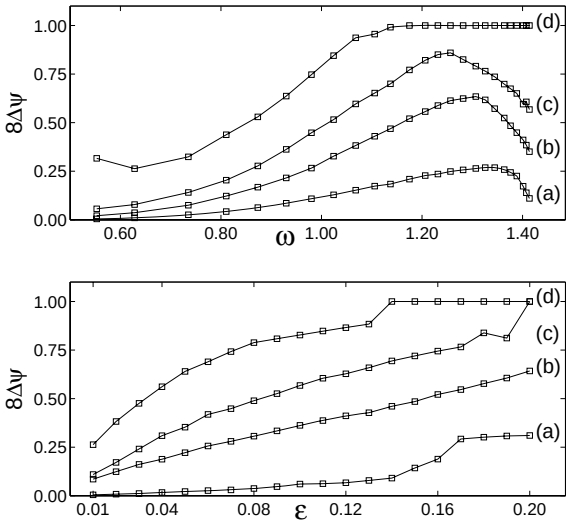

FIG. 5: Size of the chaotic mixing region; upper panel: Normalized $\Delta\psi$ *vs.* ω for the amplitudes (a) $\varepsilon = 0.01$, (b) $\varepsilon = 0.05$, (c) $\varepsilon = 0.10$, (d) $\varepsilon = 0.20$; lower panel: Normalized $\Delta\psi$ *vs.* ε for (a) $\omega = 0.55$, (b) $\omega = 0.93$, (c) $\omega = 1.28$, (d) $\omega = 1.41$.

corresponding tori $\mathcal{T}_\psi$. In between, the middle trajectory deviates much further from its $\mathcal{T}_\psi = \mathcal{T}^{(1)}(\omega)$ and fills the entire CMR. The quantity $\Delta\psi$ is probably the most convenient quantity to use in order to define the size of the CMR (around $\mathcal{T}^{(1)}(\omega)$ for $\omega < \sqrt{2}$). Computing the volume between the tori $\mathcal{T}_{\psi^-}(\omega)$ and $\mathcal{T}_{\psi^+}(\omega)$ gives the size of the CMR in the original 3D space.

The dependence of the size of the CMR (in terms of $\Delta\psi$) on ε and ω is illustrated in Fig. 5. The curves (a)-(d) in the upper and lower panels of this figure correspond to the panels (a)-(d) in Figs. 2 and 3, respectively. For a given ω value (i.e. for a given location of $\mathcal{T}^{(1)}(\omega)$), the size can be controlled by adjusting the value of ε; for example in the range of frequencies $1.181 \leq \omega \leq 1.357$, the entire droplet exhibits chaotic mixing for $\varepsilon \geq 0.175$. For each smaller value of ε the size reaches a maximum for a certain value $\omega^m(\varepsilon)$ of the frequency. On the one hand, this property can be used as an optimization technique to obtain the maximal CMR size one can reach for a given amplitude ε of the rotation. On the other hand, $\Delta\psi$ versus ε increases quite monotonically for all values of ω. Keeping in mind the brevity of the present letter, the derivation of the location of the maxima and the estimates of $\Delta\psi$ as a function of the parameters will be published elsewhere.

The structure of the CMR in this problem is rather different from that obtained in other problems that possess resonance-induced chaotic advection. Namely, in the current problem the size of the CMR goes to zero as ε goes to 0 and the CMR is localized near the resonance. In contrast, in the flow considered in, e.g., [16], the mixing is caused by resonances, but the CMR occupies a volume on the scale of the whole system. The difference comes from the fact that the averaged change of the frequency of the fast system vanishes in the current system, thus making the trajectories starting away from the resonance not being able to approach it. This property makes the kind of flows investigated in this letter very useful as it may be advantageous to localize the mixing in certain parts of the system only.

In summary, we have shown that by applying a judicious oscillatory rotation to a translating spherical drop (an integrable system), it is possible to create a chaotic mixing zone with a prescribed location and size. The appropriate values of the parameters of the perturbation (here, a rotation of a given frequency and amplitude) are determined by quantitative features of the integrable case. For a given amplitude of the rotation, the frequency optimizing the CMR size has been obtained. Such an optimization could be useful in guiding the design of practical mixing devices aiming at the best possible mixing rate within individual drops.

This letter is based upon work partially supported by the NSF (grants CTS-0626070 (N.A.), CTS-0626123 (P.S.) and 0400370 (D.V.)). D.V. is grateful to the RBRF (grant 06-01-00117) and to the Donors of the ACS Petroleum Research Fund. C.C. acknowledges support from Euratom-CEA (contract EUR 344-88-1 FUA F).

[1] H. Song, J. D. Tice and R. F. Ismagilov, Angew. Chem. int. Ed. **42**, 768 (2003)
[2] I. Glasgow and N. Aubry, Lab on a Chip **3**, 114 (2003).
[3] A. Goullet, I.K. Glasgow and N. Aubry, Mech. Res. Commun. **33**, 739 (2006).
[4] M.A. Stremler, F.R. Haselton and H. Aref, Phil. Trans. Royal Soc. A **362**, 1019 (2004).
[5] M.H. Oddy, J.G Santiago, J.C. Mikkelsen, Anal. Chem. **73**, 5822 (2001).
[6] A. Ould El Moctar, N. Aubry and J. Batton, Lab on a Chip **3**, 273 (2003).
[7] K. Bajer and H.K. Moffatt, J. Fluid Mech. **212**, 337 (1990).
[8] D. Kroujiline and H.A. Stone, Physica D **130**, 105 (1999).
[9] T. Ward and G.M. Homsy, Phys. Fluids **13**, 3521 (2001).
[10] S.M. Lee, D.J. Kim and I.S. Kang, Phys. Fluids **12**, 1899 (2000)
[11] R.O. Grigoriev, M.F. Schatz and V. Sharma, Lab Chip, **6**, 1369 (2006).
[12] T. Solomon and I. Mezic, Nature **425**, 376 (2003). (2007).
[13] M. Feingold, L. Kadanoff and O. Piro, J. Stat. Phys. **50**, 529 (1988).
[14] D. Vainchtein, A. Vasiliev and A. Neishtadt, Chaos **6**, 67 (1996).
[15] D. Vainchtein, A. Neishtadt and I. Mezic, Chaos **16**, 043123 (2006).
[16] D. Vainchtein, J. Widloski and R. Grigoriev, Phys. Rev. Lett., in press (2007).